~~CONFIDENTIAL~~

Copy
RM E57K19b

RESEARCH MEMORANDUM

INVESTIGATION AT SUPERSONIC SPEEDS OF THE COMPRESSOR STALL AND INLET BUZZ CHARACTERISTICS OF A J34 - SPIKE-INLET COMBINATION

By J. Cary Nettles and Robert C. Campbell

Lewis Flight Propulsion Laboratory
Cleveland, Ohio

CLASSIFIED DOCUMENT

NATIONAL ADVISORY COMMITTEE
FOR AERONAUTICS

WASHINGTON
March 5, 1958

~~CONFIDENTIAL~~

NACA RM E57K19b

NATIONAL ADVISORY COMMITTEE FOR AERONAUTICS

RESEARCH MEMORANDUM

INVESTIGATION AT SUPERSONIC SPEEDS OF THE COMPRESSOR STALL AND INLET BUZZ CHARACTERISTICS OF A J34 - SPIKE-INLET COMBINATION

By J. Cary Nettles and Robert C. Campbell

SUMMARY

The investigation of the interactions that occur when a supersonic diffuser is operated with a turbojet engine was extended by installing a variable-area exhaust nozzle on a J34 engine to permit the attainment of limiting engine temperature or compressor pressure ratio at all engine speeds. For a Mach number range from 1.6 to 2.0 and angles of attack from 0° to 9° the results indicated that the occurrence of engine stall was determined by inlet operating conditions because of the flow profile presented to the compressor. The occurrence of stall was related to a pressure deficiency at the hub of the compressor and was not predicted by the distortion parameter. The referred engine airflow tended to increase as the radial distortion level increased.

Approaching the inlet buzz limit with an engine operating in or near stall did not affect the minimum stable airflow of the diffuser, and conversely the presence of mild buzz did not affect the compressor stall limit.

The stability limits of a double-cone inlet having 15° plus 10° half-angles were essentially the same with the engine as with a choked plug.

INTRODUCTION

In order to realize the full performance potential of a combination of supersonic diffuser and turbojet engine, it is necessary that the characteristics of the two be compatible. Even when the stall and buzz margin of each component appears satisfactory by itself, other operating limits may exist for the combination because of interaction of one unit upon the other. For instance, compressor stall and inlet buzz are similar phenomena, and therefore, when they are coupled together, the dynamic system response might range from mutual excitation to mutual damping. In addition, the stall limits of the engine can be influenced by the flow profile that the inlet presents to the compressor face.

Investigations of the operating characteristics of an adjustable supersonic inlet and a J34 engine are reported in references 1 and 2. These investigations were made with an engine having a fixed-area nozzle and operating conditions well removed from compressor stall. The scope of the previous work was extended for the present investigation by utilizing a different model of the J34 and a variable-area nozzle so that the engine could be made to stall. The buzz and stall limits of the inlet-engine combination were determined for various operating conditions. In certain cases points were obtained during which buzz and stall were occurring simultaneously.

The results reported herein were obtained in the Lewis 8- by 6-foot supersonic wind tunnel during February, 1956. The investigations were conducted for a Mach number range from 1.6 to 2.0 and angles of attack from 0° to 9°.

APPARATUS AND INSTRUMENTATION

The nacelle and inlet used for this investigation are essentially the same as those reported in reference 1. The general layout is shown in figure 1(a). A variable bypass and a translating spike allowed a wide flexibility for matching inlet characteristics to the engine requirements. A variable-area exhaust nozzle was installed on the engine to allow additional control of turbine-inlet temperature. For most of the test a turbine-flow-area restrictor was installed ahead of the first turbine stator to provide higher compressor back pressure without exceeding turbine temperature limits. The restrictor was a simple flat ring welded around the inner radius of the stator and blocking an estimated 30 percent of the geometric area. The nacelle mounting strut allowed the entire unit to be rotated to a 9° angle of attack. Figure 1(b) is a photograph of the model installed in the tunnel.

The diffuser design allowed the 25° half-angle spike to be translated so that the conical shock could intersect the cowl lip for Mach numbers from 2.4 to 1.58 without encountering internal contraction. The flow-area variation of the subsonic diffuser is shown in figure 2 for the limits of spike travel.

The 15° half-angle cone extension of reference 3 was installed during part of the test program to determine the stability limits of the two-oblique-shock diffuser with an engine.

Inlet flow conditions were surveyed at two stations in the inlet. At a plane 28 inches aft of the cowl lip, ahead of the bypass slots, the instrumentation consisted of four rakes of five total-pressure tubes each, mounted between the four struts supporting the centerbody. The tubes were spaced radially to provide an area-weighted average. Static

pressures were measured near the base and tip of each rake. The conditions associated with the diffuser discharge were evaluated at a plane 58 inches aft of the cowl lip, about 10 inches upstream of the engine guide vanes. The diffuser-discharge instrumentation consisted of eight rakes of eight tubes each. The rakes were located at 45° intervals starting from the top, and the tubes were spaced radially according to equal areas. Static pressures were measured on the outer wall near each rake.

Compressor-discharge pressure was measured by four rakes of four tubes each, which were mounted through existing access holes in the compressor case. The ends of the compressor-discharge measuring tubes were unavoidably close to a row of mixing blades that are a part of the compressor assembly. It was felt that in spite of this a representative average discharge pressure was obtained.

Referred airflow was computed from average total and static pressure and an assigned flow area. The diffuser-discharge instrumentation was used in all cases to determine the engine referred airflow. For cases where the bypass was open, the diffuser capture airflow was computed from the instrumentation at the 28-inch position. This method of determining the referred airflow suffers in terms of absolute accuracy because of the difficulty of defining the true flow area. Relative values of referred airflow are generally consistent and reliable.

Static-pressure transducers were installed at various stations along the diffuser and engine in order to get a time history of pressure disturbances throughout the system. The transducer stations were located: 1/2 inch inside the cowl lip, about midway between the cowl lip and the compressor face, at the diffuser-discharge station, at the third-stage rotor, at the fifth-stage rotor, at the compressor discharge, and in the cylindrical section of the tailpipe. A simultaneous record of the pressure fluctuations throughout the system was obtained by recording the outputs of the transducers on a multichannel optical oscillograph having galvanometers with a 100 cps cutoff frequency.

RESULTS AND DISCUSSION

Engine Stall Limits

A calibration of the engine compressor was made at a tunnel Mach number of 1.7 and with a spike position M_d of 1.6. (Symbols are defined in the appendix.) The inlet was known from previous work to be free of buzz for the conditions selected. The data for this compressor calibration are presented in figure 3. Two points taken at a Mach number of 0.55 are included to increase the range of the data. The variable-area nozzle used to vary back pressure on the engine did not permit an accurate determination of the flow area. As a result, the nominal nozzle

areas on figure 3 and following figures have no significance other than to indicate order of magnitude and that the nozzle position was constant. For all engine speed ratios up to the maximum mechanical speed of the engine, it was possible, by closing the exhaust nozzle, to obtain the maximum allowable turbine-inlet temperature without encountering engine stall. (The connotation of the words engine stall is taken in this report to be any disturbance to the flow believed to originate within the engine.) For any given engine speed ratio the compressor pressure ratio increases and the referred airflow decreases as the nozzle area is reduced.

The compressor calibration was repeated with a spike position M_d of 1.8. The results are presented in figure 4. With this spike position it was found that engine stall was encountered for engine speed ratios less than 0.8 and compressor pressure ratios well below the maximum values indicated on figure 3. A check of the engine stall limit was determined with an inlet spike position of 2.4, and it was found that essentially the same stall limit existed for this spike position as for $M_d = 1.8$. The data in figure 4 indicate that the stall limit developed in such a way that reducing the referred engine speed with the nozzle area that gives rated turbine-inlet temperature would drive the compressor into stall.

Oscillograph traces of the engine stall pressure disturbance are shown in figure 5. Figure 5(a), which is a trace taken for point A of figure 4, is of particular interest because for this condition the stall disturbance was apparent from visual observation as an intermittent jumping of the inlet terminal shock between what appeared to be two stable positions. An inspection of the oscillograph traces indicates that a jump in cowl lip pressure corresponds to the buildup of a high-frequency disturbance of the compressor third-stage static pressure. This high frequency corresponds to one-half engine speed and could originate from rotating stall. During the high-frequency disturbance the cowl-lip static pressure oscillates with a low-frequency underdamped response. Finally the high frequency dies down and the cowl-lip pressure jumps back to its initial value.

This same sequence of events can be envisioned for the traces shown in figures 5(b) and (c) (points B and C of fig. 4); however, for these cases the phenomena is recurring at a regular rate. The indicated low frequency of these traces is in fact of the same order as the inlet buzz frequency. This raises the immediate question of how stall or buzz can be identified from the oscillograph trace. During this investigation identification of the disturbance taking place had to be based on the corrective action required to eliminate the disturbance. In the cases called engine stall, changing the inlet conditions by means of the bypass or spike position had no effect on the disturbance, except for a radial profile effect discussed later, whereas increasing the exhaust-nozzle size even a small amount eliminated the disturbance.

Radial profiles of total-pressure recovery representative of the flow approaching the entire engine face are shown in figure 6 for conditions where stall was encountered and for a typical case from the data of figure 3 where maximum turbine temperature was obtained without stall. These profiles indicate that stall was encountered when there was a radial distortion of the flow. In particular, the stall appears to have been related to the presence of a pressure deficiency in the flow near the hub.

An attempt to combine the data of figures 3 and 4 into a single compressor performance map was not successful because the radial flow distortion caused a shift of compressor flow at any given referred speed and pressure ratio. The indicated shift in compressor flow is shown in figure 7, where referred flow is used as the common abscissa for the two sets of data. Parts of figure 7 were constructed from data and extrapolations which are not shown in figures 3 and 4. These are indicated by the broken lines in the figure. For referred speeds below 0.90 the compressor flow is greater with distorted flow than without. For speeds above 0.90 the flow appears to be reduced, but this fact is not well established by the data.

4366

In figure 8 data are presented for selected conditions of constant compressor pressure ratio and referred engine speed ratio. These data indicate that in general the compressor airflow increases with distortion level. It should be noted, however, that the variable distortion level was achieved by varying the inlet spike position, and, therefore, all the profiles are similar, that is, have a pressure deficiency at the hub. The trend observed in the data is not illogical, because for a given average condition, such as constant pressure ratio and referred speed ratio, a pressure decrement in the flow tends to increase the blade-life coefficient more than the same amount of pressure increment would decrease the lift coefficient; therefore, the total work input of the stage can increase with distortion level. This is, of course, the same mechanism that causes the engine to stall.

Independent checks made from fuel flow and from turbine pressure ratio indicated that the changes in airflow were real and were not just a result of the method used to compute airflow.

Figure 9 presents the engine stall limits that were determined at a tunnel Mach number of 1.8 with a spike setting M_d of 2.3. The stall limit near a speed ratio of 0.8 is essentially the same as determined at an M_0 of 1.7. However, the stall limit at a speed ratio of 0.745 is lower than for the previous data. The radial profiles for these stall points are presented in figure 10. Comparison of the profiles of figure 10 with the profiles of figure 6 indicates that the distortion levels are slightly higher; but the form of the distortion for the speed condition near 0.75 is considerably different. The 1.8 data point has more low-pressure area in the vicinity of the hub, and this could account for the

lower stall pressure ratio. A typical oscillogram of an engine stall disturbance at an M_0 of 1.8 is shown in figure 11. The indicated sequence of events is the same as described for figure 5(a).

A series of runs was made at maximum compressor pressure ratios, a Mach number of 2.0, and a nominal referred speed of 0.80 for a range of spike positions. The results are presented in figures 12 and 13. The stall limit appears to be independent of spike position above a spike setting of 1.9. At a spike setting of 1.8, however, the stall limit was not reached at the limiting turbine-inlet temperature. An inspection of the profiles presented in figure 13 indicates that, even though the distortion parameter was about the same, a marked change in the flow occurred between spike settings of 1.9 and 1.8; in fact, the form of the distortion had reversed at 1.8 so that the high pressure appeared at the hub. Throughout these data there is no apparent correlation between the distortion parameter $\Delta P/P_3$ and the occurrence of stall.

The effect of angle of attack on the stall pressure ratio is presented in figure 14 for a spike position of 2.4. The resulting radial profiles indicated by rakes in an upper and lower quadrant are shown in figure 15. The angle-of-attack data indicate that superimposing a circumferential distortion on the radial distortion did not alter the stall pressure ratio. A similar test could not be run with a distortion profile that did not stall at zero angle of attack because it was not possible to avoid the inlet buzz limit at angle of attack.

Inlet Stability Limits

The stability limits of the diffuser were checked for the most part with the unmodified engine. These data are presented in figure 16. At each particular spike position the stability limit was determined with the engine operating with the minimum compressor pressure ratio (nozzle open) and with the maximum pressure ratio (nozzle closed). Within the limits of the data, there was no indicated effect of engine operating condition on the stability limits. With the modified engine it was possible to run a few points for which the stability limit and the stall limit were coincident. These data are also presented in figure 16 and indicate that the presence of a stall disturbance which in itself was causing transient shock movements did not affect the stability limit of the diffuser. An oscillogram of the simultaneous stall and buzz disturbance occurring at the point designated A in figure 16 is presented in figure 17. A check of the engine stall pressure ratios at the minimum stable points indicated that they were consistent with the previous data.

The stability limits of the two-oblique-shock inlet of reference 3 as determined with the engine are presented in figure 18. Comparison of

the present data with the previous cold-pipe data with allowance made for the apparent difference in critical referred airflow indicates that the presence of the engine had no significant effect on the stability limits. The data at the 9° angle of attack are beyond the range of the data of reference 3 but are included to show the stability characteristics of this inlet at the higher angle.

CONCLUSIONS

The test results of an inlet-engine combination consisting of a translating-spike inlet with a bypass diffuser, a J34 engine, and a variable-area nozzle operated at Mach numbers from 1.6 to 2.0 indicate the following:

1. Because the radial profile of total pressure delivered to the compressor face varied with spike position, operating conditions for the inlet-engine combination ranged from complete freedom from engine stall to stall within the normal operating range with fixed nozzle area.

2. No correlation between the distortion parameter and the occurrence of stall was found. The occurrence of stall was related to the presence of a pressure deficiency at the hub of the compressor.

3. The referred engine airflow tended to increase at a given referred engine speed as the radial distortion level increased.

4. Superimposing a circumferential distortion on a radial distortion by changing the inlet angle of attack did not affect the stall-limited compressor pressure ratio.

5. Approaching the buzz limit of the inlet with an engine in or near stall did not affect the minimum stable airflow of the diffuser.

6. The stability limits of a 15° plus 10° double-cone inlet were essentially the same with the engine as with a choked plug.

Lewis Flight Propulsion Laboratory
National Advisory Committee for Aeronautics
Cleveland, Ohio, November 20, 1957

APPENDIX - SYMBOLS

A area, normal to flow

A_c inlet capture area

D_h hydraulic diameter, $\frac{4A}{\text{wetted perimeter}}$

M Mach number

M_d Mach number at which conical shock intersects cowl lip

N engine rotational speed, percent of rated

P total pressure

$\frac{\Delta P}{P}$ flow-distortion parameter, $\frac{P_{max} - P_{min}}{P_{av}}$

w airflow

δ ratio of total pressure to NACA standard sea-level pressure of 2116 lb/sq ft

θ ratio of total temperature to NACA standard sea-level temperature of 518.7° R

Subscripts:

x axial station

0 free stream

1 cowl lip

2 diffuser discharge

3 compressor discharge

4366

REFERENCES

1. Nettles, J. C., and Leissler, L. A.: Investigation of Adjustable Supersonic Inlet in Combination with J34 Engine up to Mach 2.0. NACA RM E54H11, 1954.

2. Beheim, Milton A., and Englert, Gerald W.: Effects of a J34 Turbojet Engine on Supersonic Diffuser Performance. NACA RM E55I21, 1956.

3. Nettles, J. C.: Investigation of the Air-Flow-Regulation Characteristics of a Translating-Spike Inlet with Two Oblique Shocks from Mach 1.6 to 2.0. NACA RM E56D23b, 1956.

[redacted]

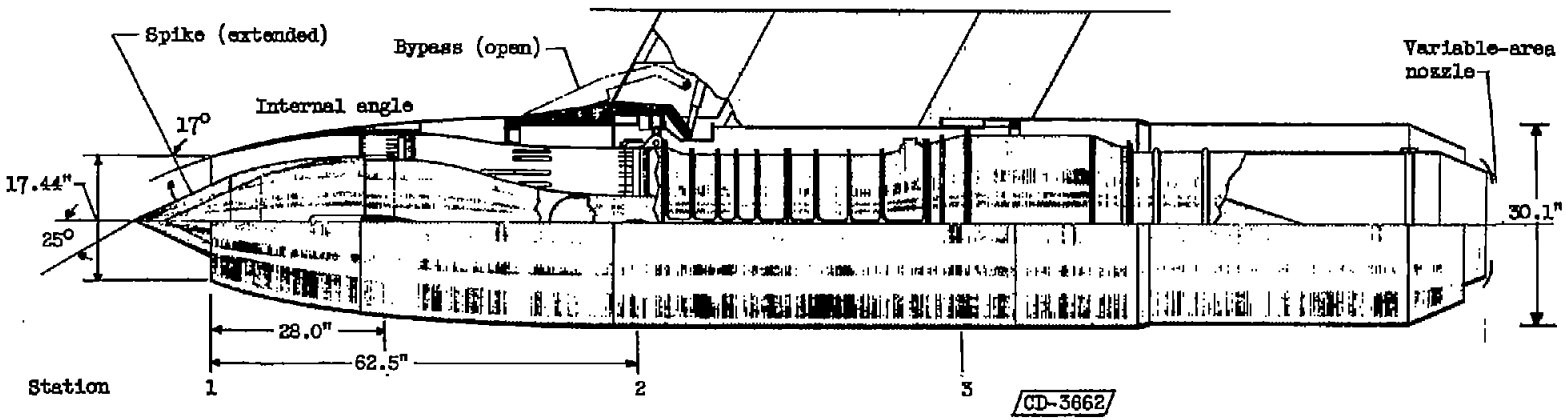

(a) General layout.

Figure 1. - Nacelle configurations.

(b) Photograph of nacelle installed in 8- by 6-foot tunnel.

Figure 1. - Concluded. Nacelle configurations.

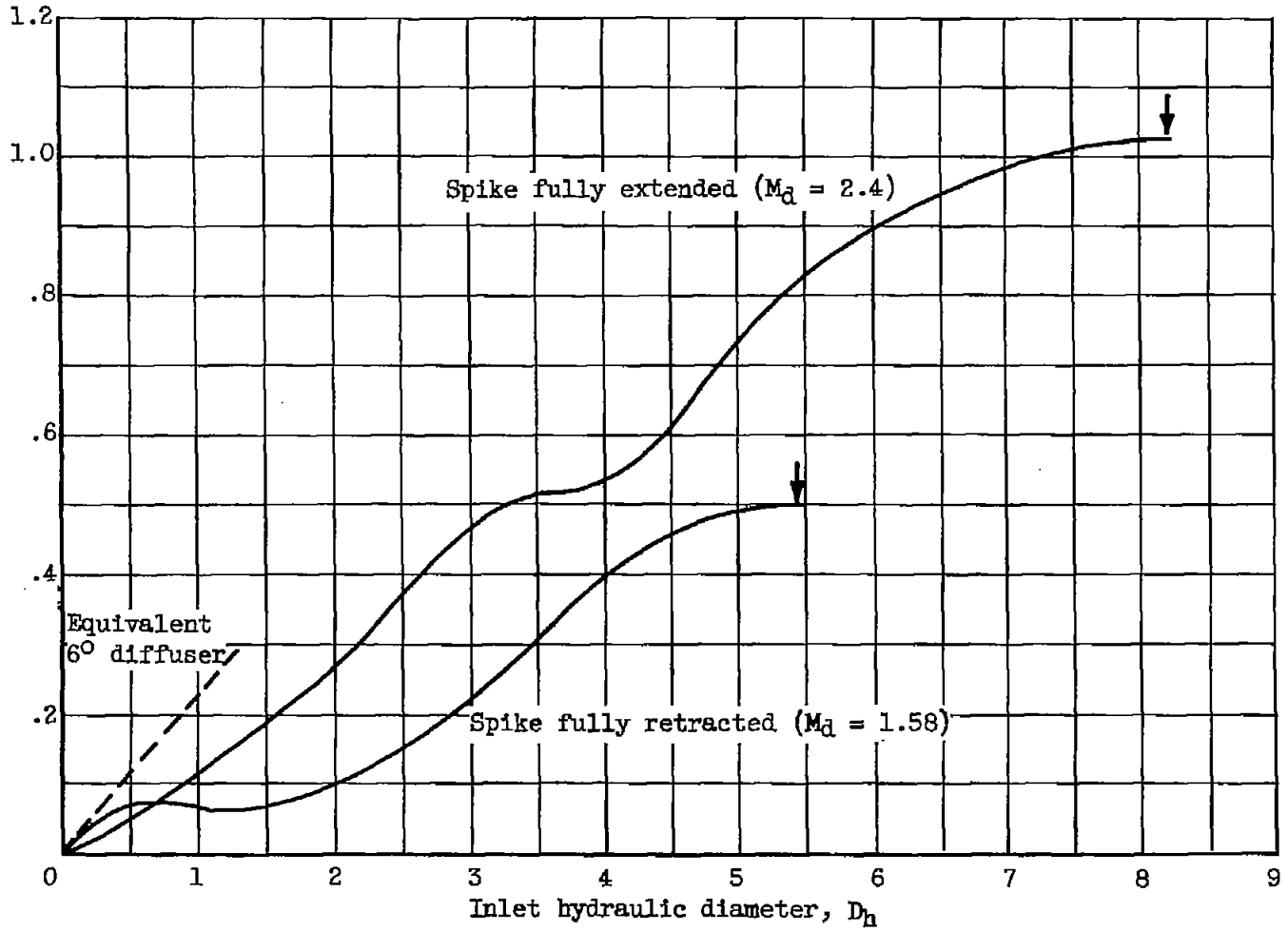

Figure 2 - Diffuser-area variation for two spike positions. M_d, Mach number at which oblique shock intersects cowl lip; arrow indicates compressor face.

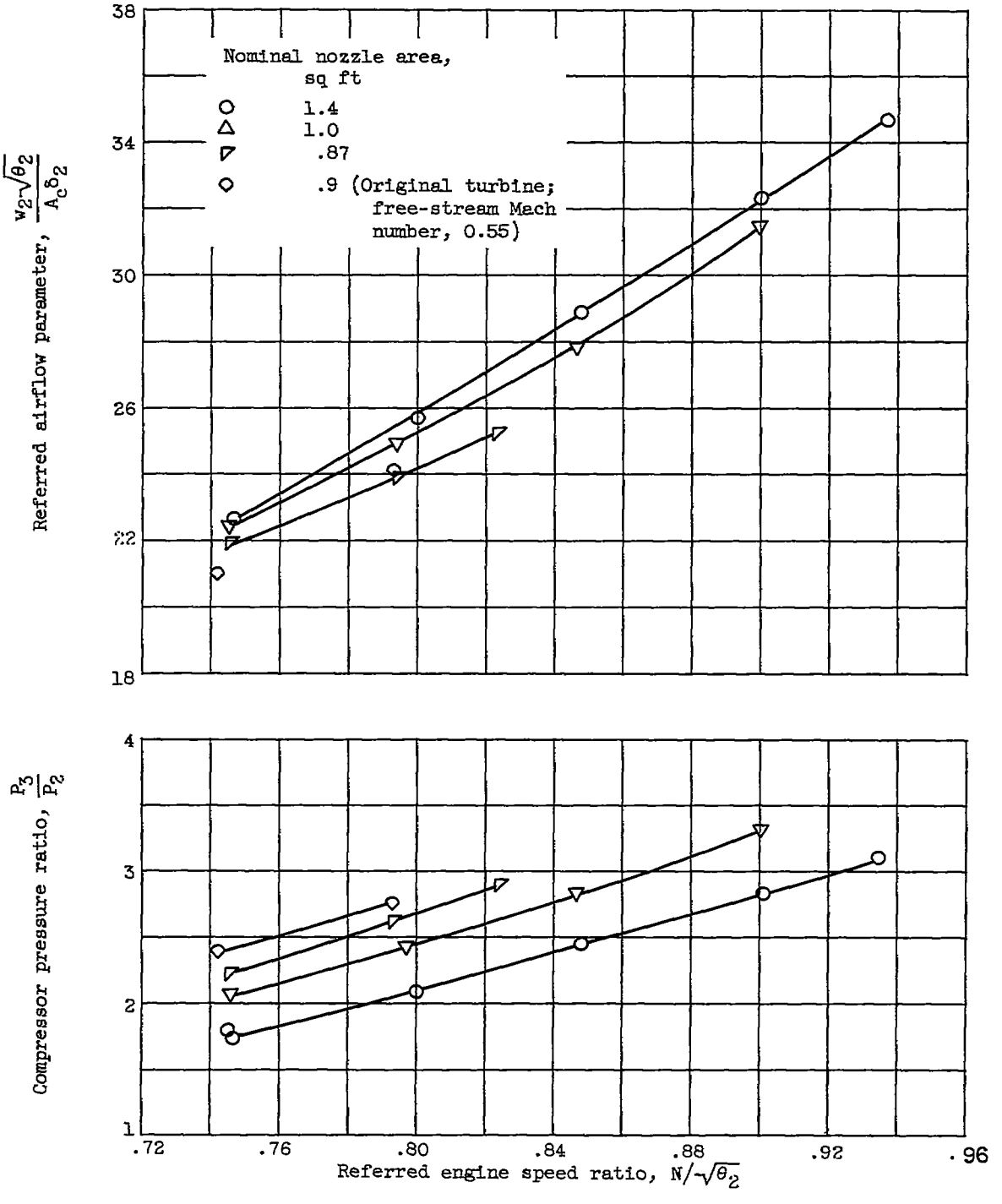

Figure 3. - Compressor performance with subcritical buzz-free inlet condition. Mach number at which conical shock intersects cowl lip, 1.6; free-stream Mach number, 1.7.

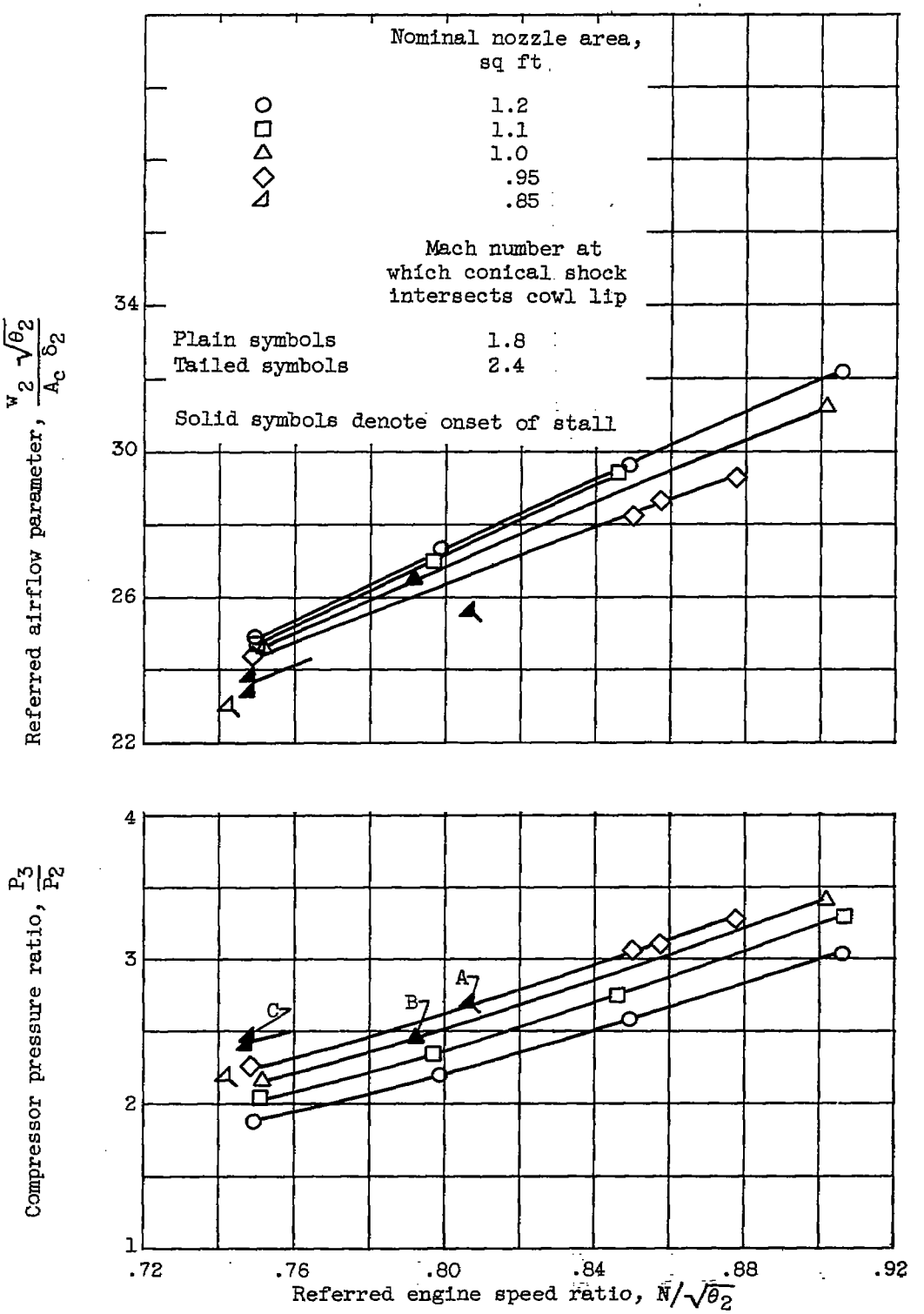

Figure 4. - Compressor performance with radial distortion at compressor face. Free-stream Mach number, 1.7.

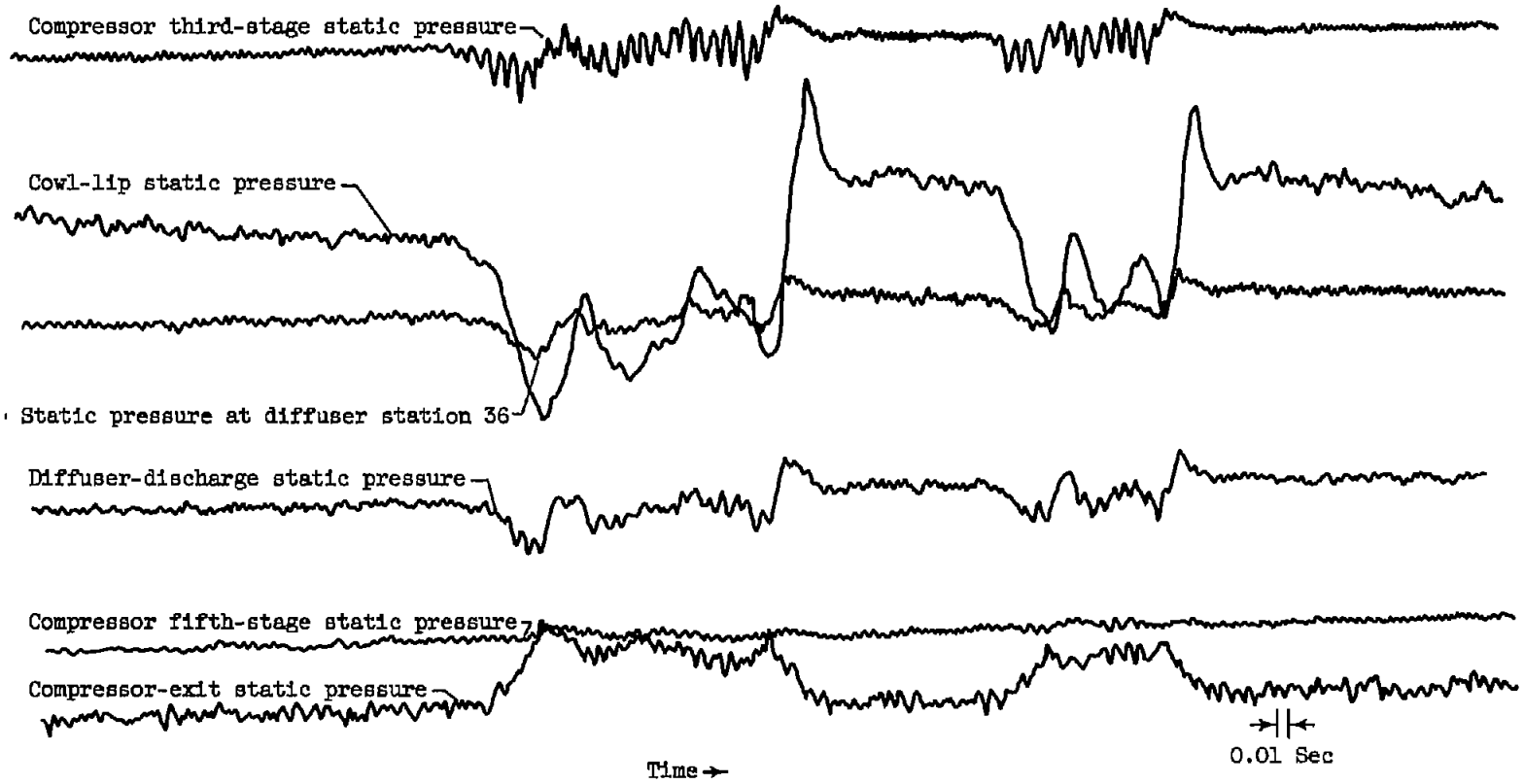

(a) Mach number at which conical shock intersects cowl lip, 2.4; referred engine speed ratio, 0.806; compressor pressure ratio, 2.68.

Figure 5. - Oscillogram of inlet-engine variables during compressor stall. Free-stream Mach number, 1.7.

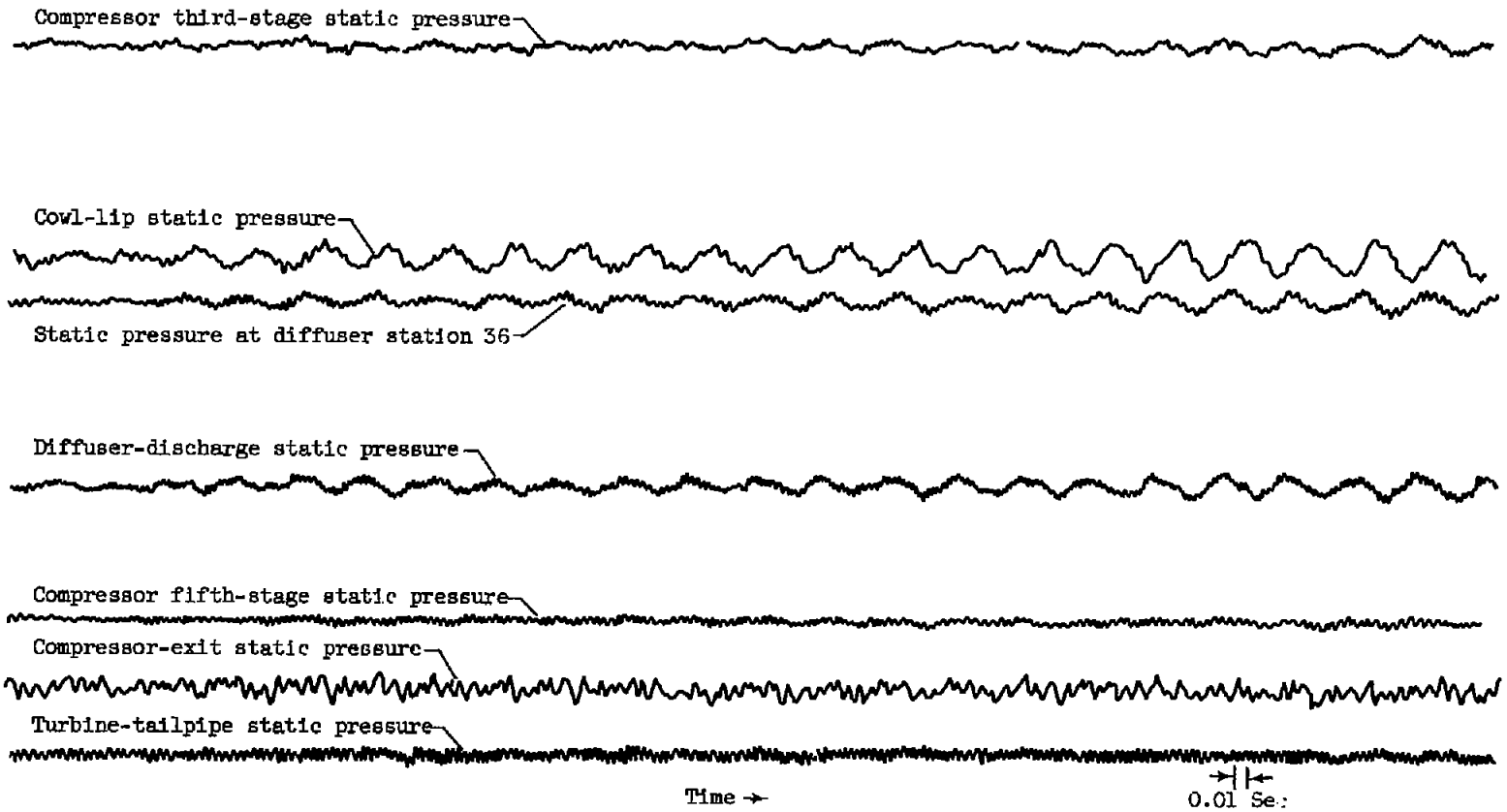

(b) Mach number at which conical shock intersects cowl lip, 1.8; referred engine speed ratio, 0.792; compressor pressure ratio, 2.45.

Figure 5. - Continued. Oscillogram of inlet-engine variables during compressor stall. Free-stream Mach number, 1.7.

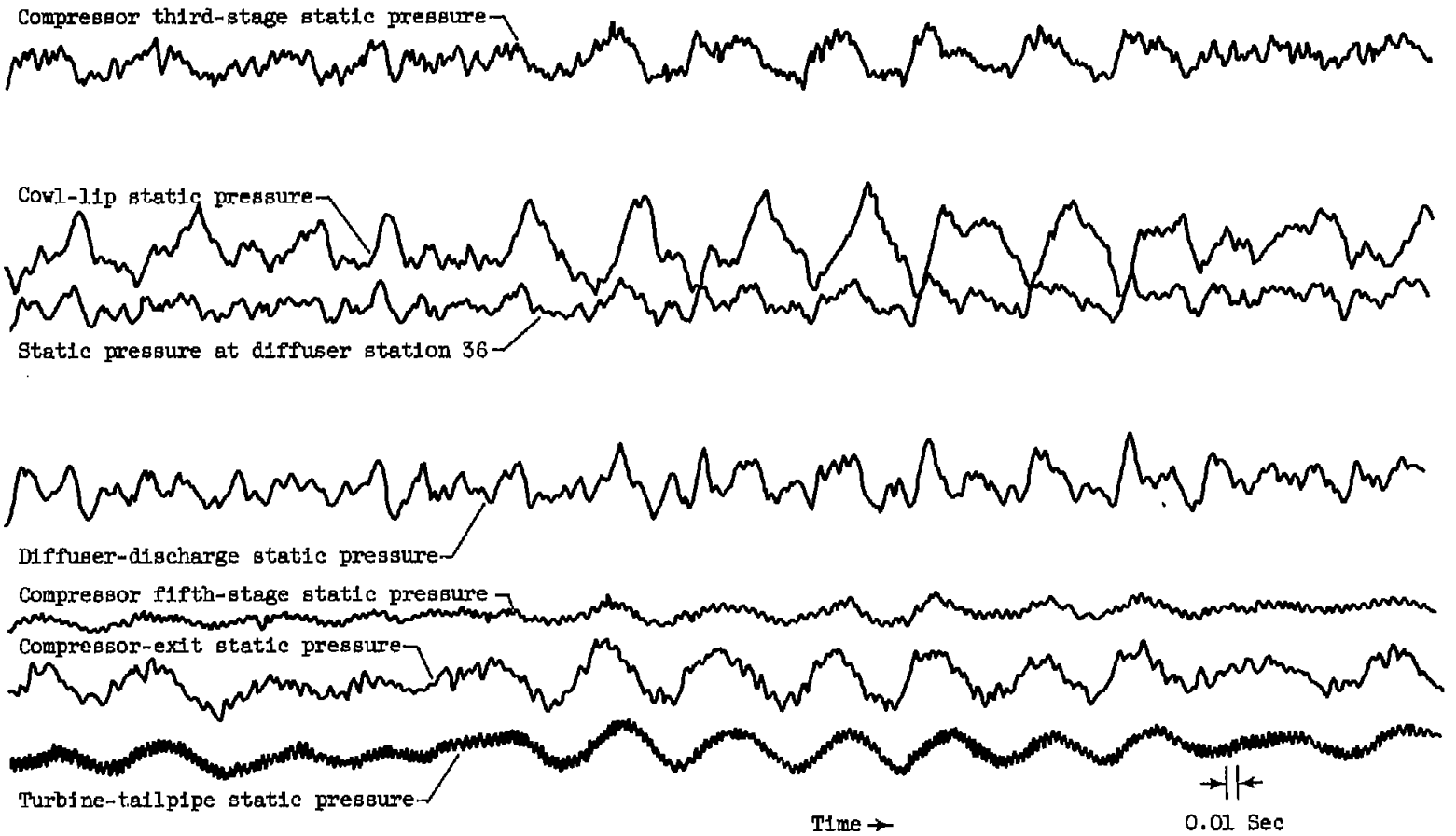

(c) Mach number at which conical shock intersects cowl lip, 1.8; referred engine speed ratio, 0.748; compressor pressure ratio, 2.45.

Figure 5. - Concluded. Oscillogram of inlet-engine variables during compressor stall. Free-stream Mach number, 1.7.

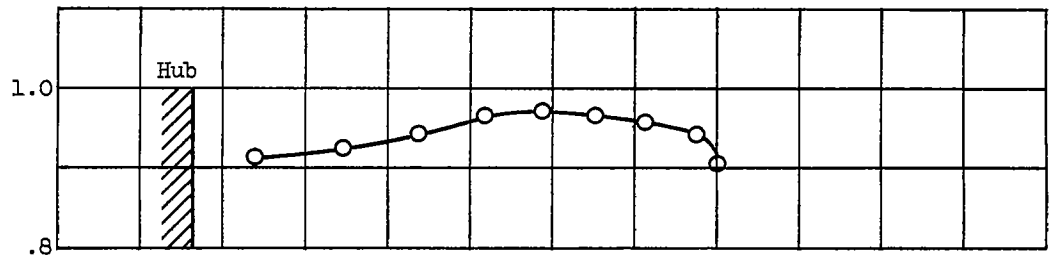

(a) Mach number at which conical shock intersects cowl lip, 2.4; referred engine speed ratio, 0.806; compressor pressure ratio, 2.68; compressor-face total-pressure distortion, 0.07; stall.

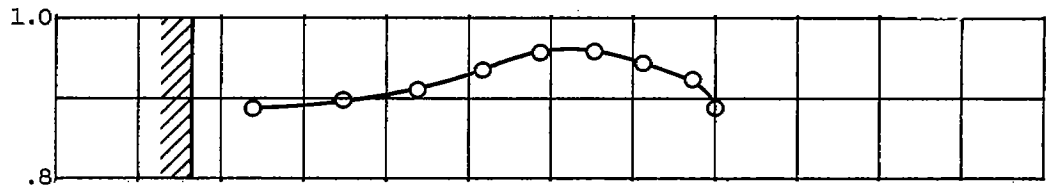

(b) Mach number at which conical shock intersects cowl lip, 1.8; referred engine speed ratio, 0.792; compressor pressure ratio, 2.45; compressor-face total-pressure distortion, 0.09; stall.

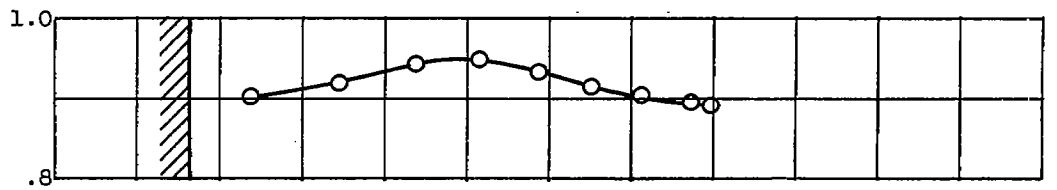

(c) Mach number at which conical shock intersects cowl lip, 1.8; referred engine speed ratio, 0.748; compressor pressure ratio, 2.45; compressor-face total-pressure distortion, 0.06; stall.

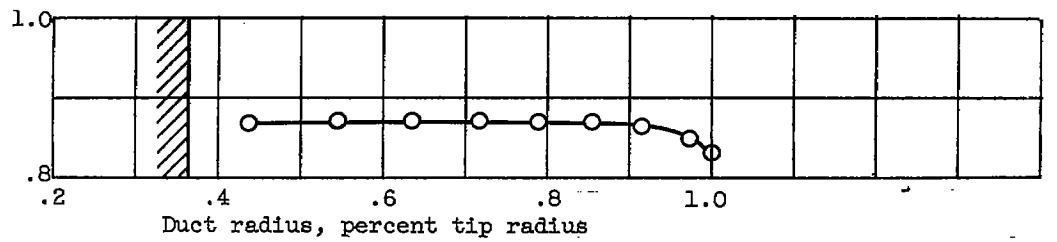

(d) Mach number at which conical shock intersects cowl lip, 1.6; referred engine speed ratio, 0.794; compressor pressure ratio, 2.61; compressor-face total-pressure distortion, 0.04; no stall.

Compressor-face total-pressure ratio, $\frac{P_2}{P_0}$

Figure 6. - Typical compressor-face total-pressure profiles. Free-stream Mach number, 1.7.

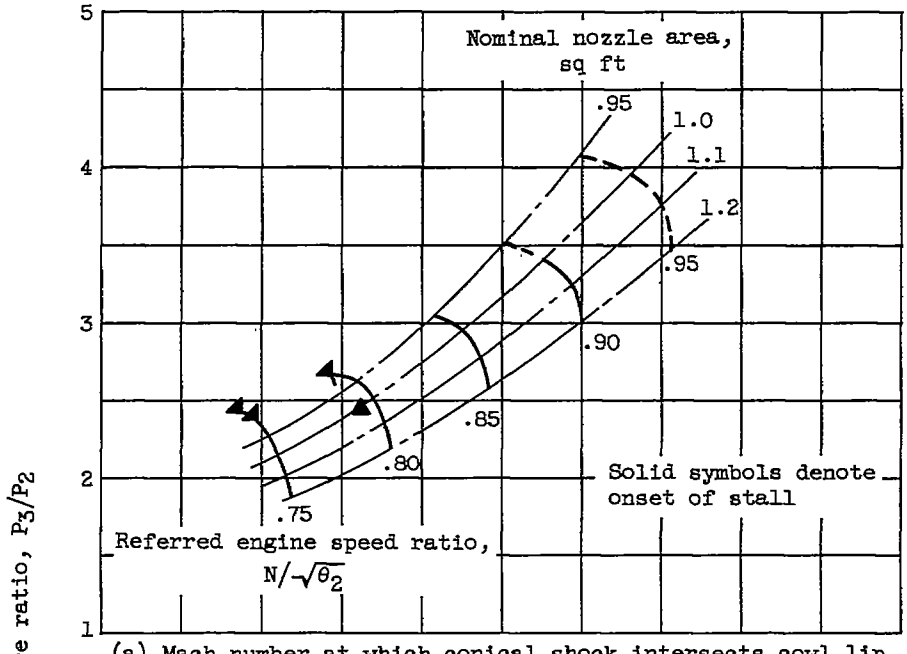

(a) Mach number at which conical shock intersects cowl lip, 1.8.

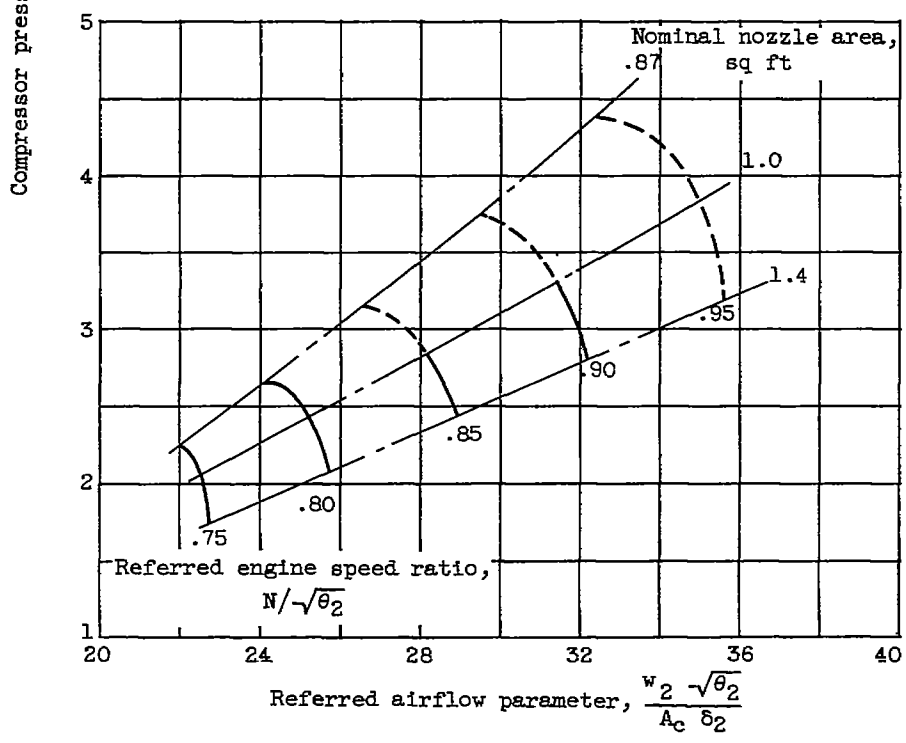

(b) Mach number at which conical shock intersects cowl lip, 1.6.

Figure 7. - Combined compressor performance. Free-stream Mach number, 1.7.

[redacted]

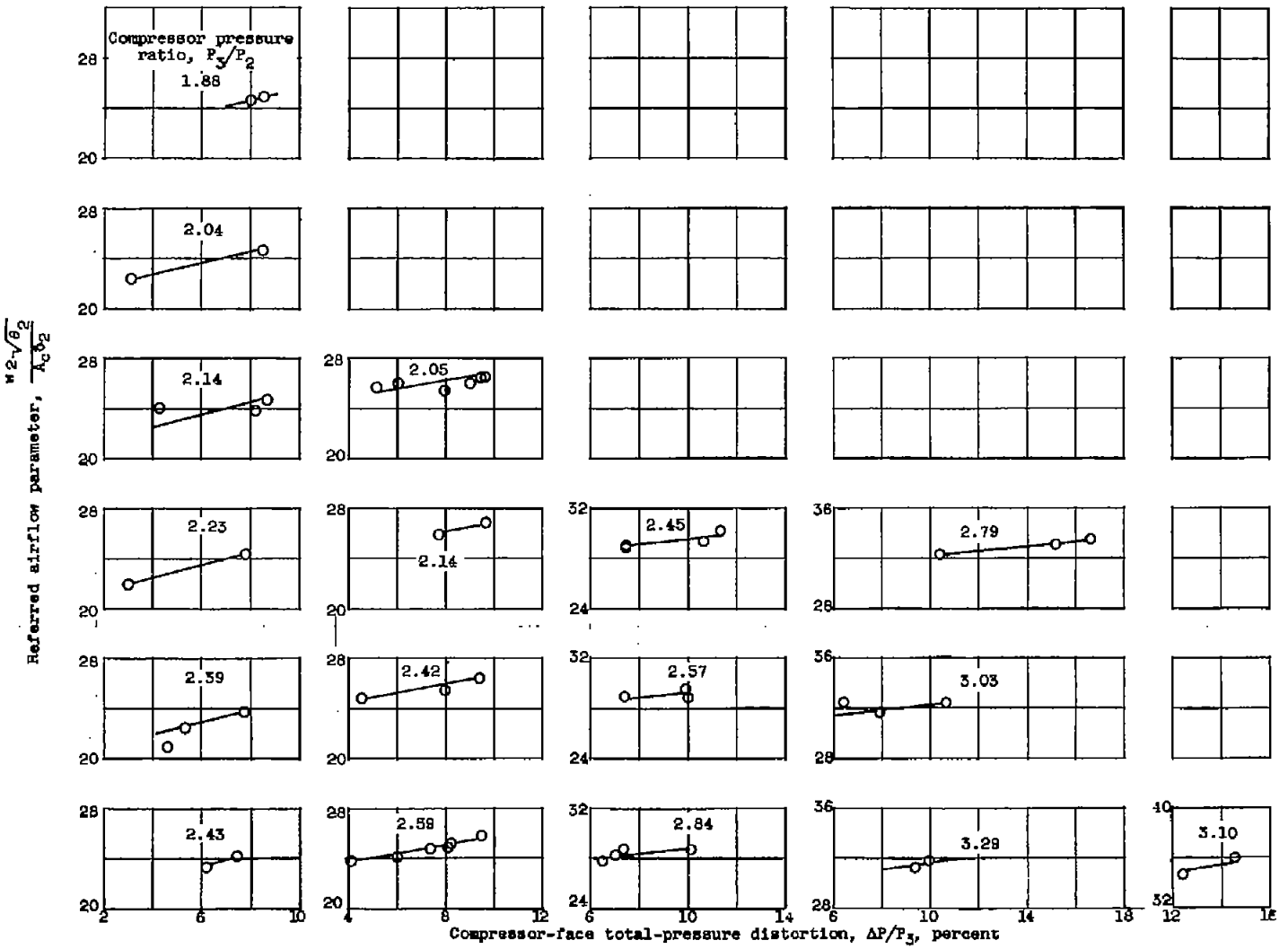

(a) Referred engine speed ratio, 0.75. (b) Referred engine speed ratio, 0.80. (c) Referred engine speed ratio, 0.85. (d) Referred engine speed ratio, 0.90. (e) Referred engine speed ratio, 0.95.

Figure 8. - Variation of referred airflow with distortion parameter.

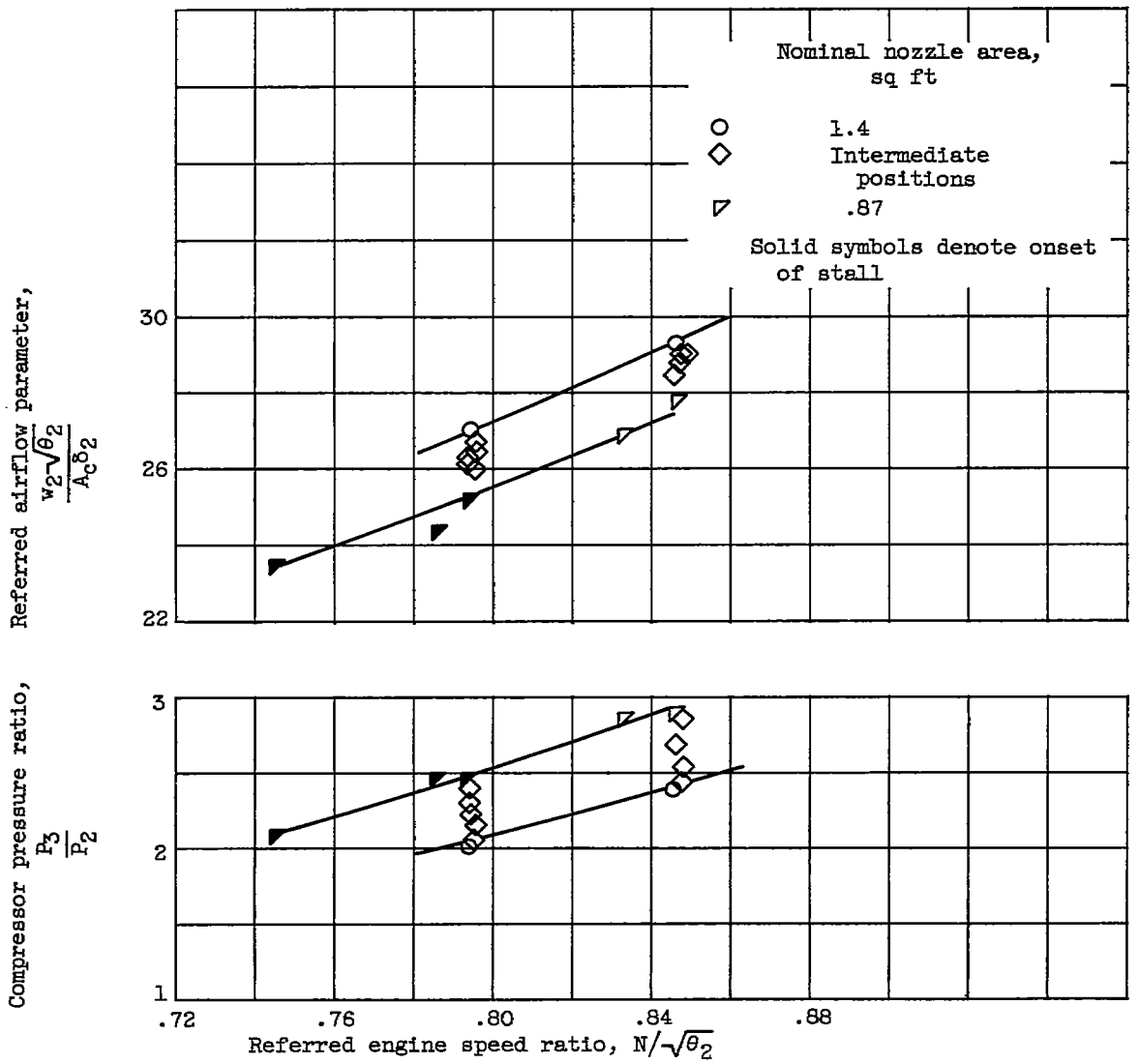

Figure 9. - Compressor performance with radial distortion at compressor face. Mach number at which conical shock intersects cowl lip, 2.3; free-stream Mach number, 1.8.

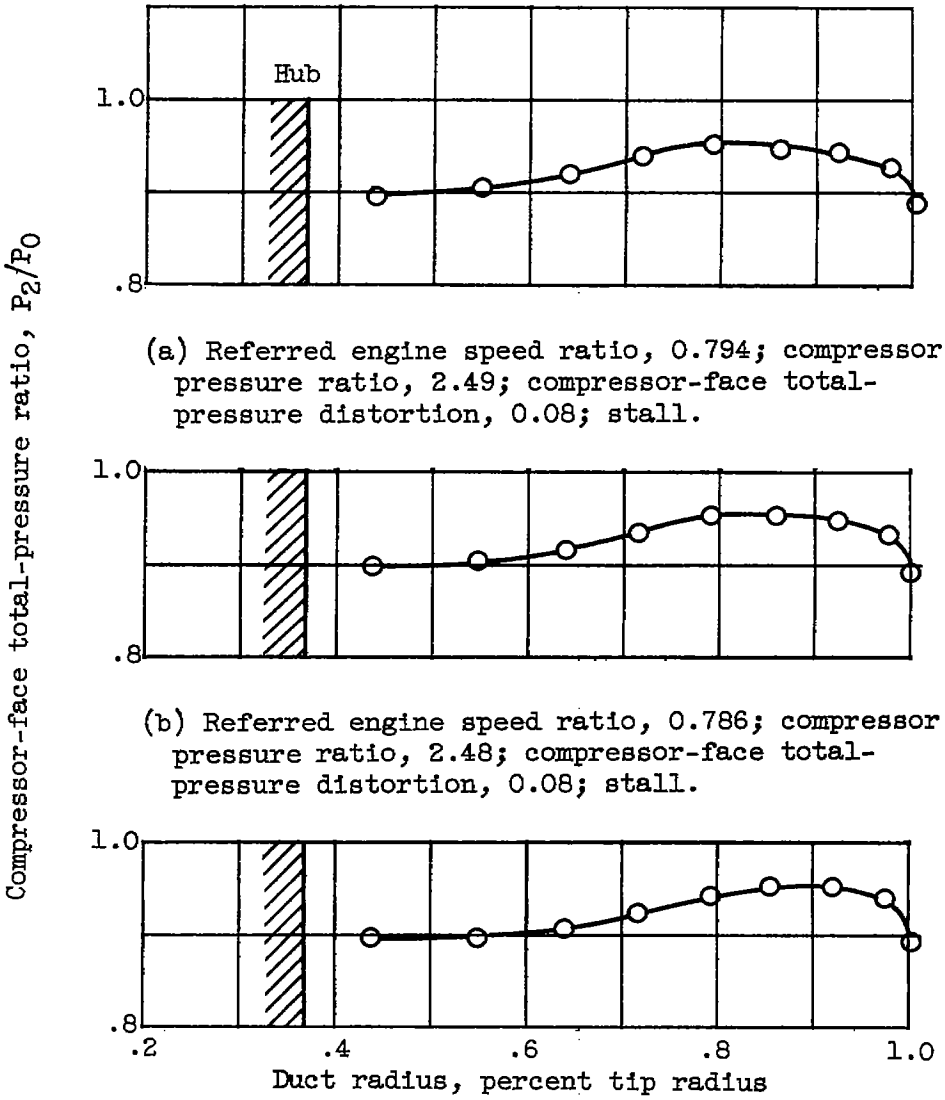

(a) Referred engine speed ratio, 0.794; compressor pressure ratio, 2.49; compressor-face total-pressure distortion, 0.08; stall.

(b) Referred engine speed ratio, 0.786; compressor pressure ratio, 2.48; compressor-face total-pressure distortion, 0.08; stall.

(c) Referred engine speed ratio, 0.745; compressor pressure ratio, 2.09; compressor-face total-pressure distortion, 0.08; stall.

Figure 10. - Typical compressor-face total-pressure profiles. Mach number at which conical shock intersects cowl lip, 2.3; free-stream Mach number, 1.8.

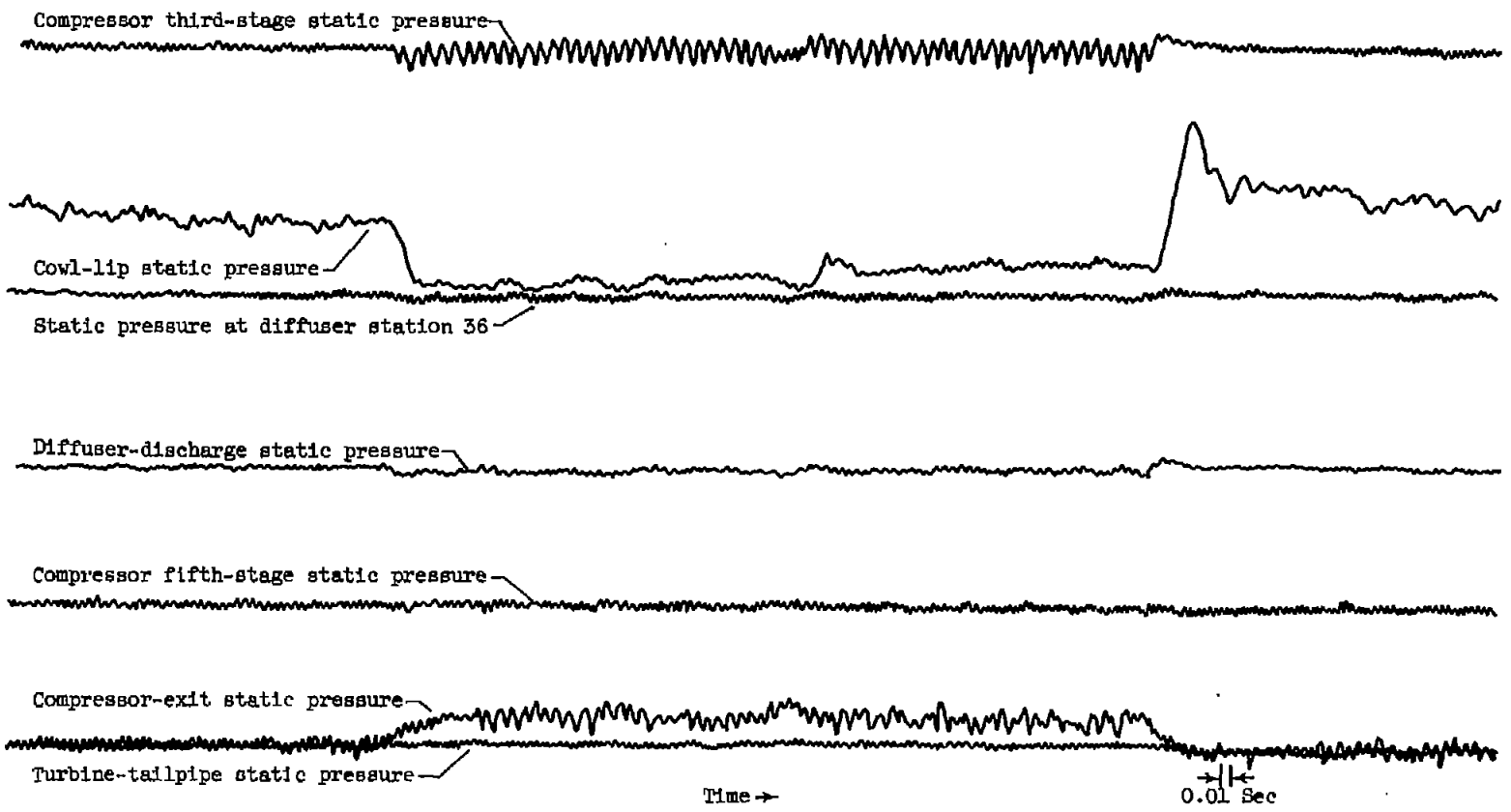

Figure 11. - Oscillogram of inlet-engine variables during compressor stall. Mach number at which conical shock intersects cowl lip, 2.3; free-stream Mach number, 1.8; referred engine speed ratio, 0.794; compressor pressure ratio, 2.49.

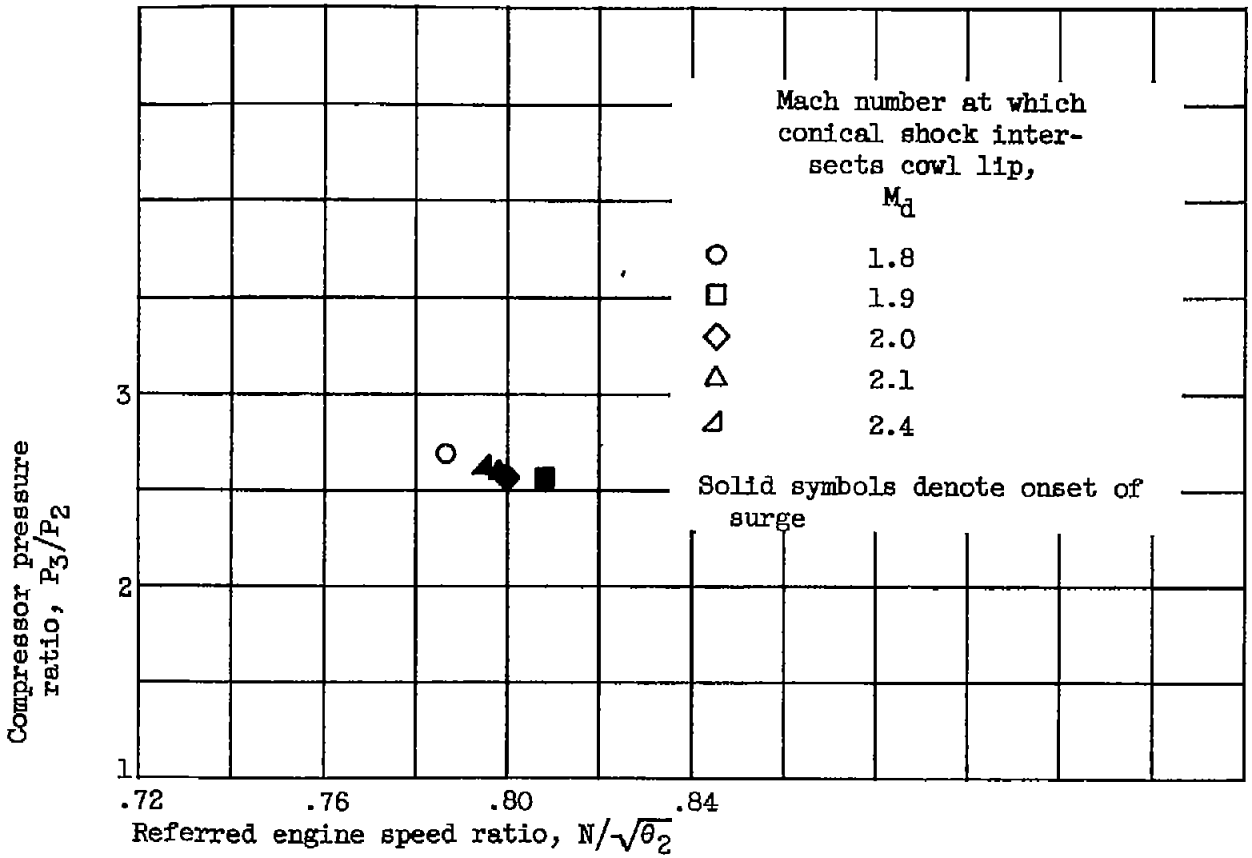

Figure 12. - Effect of inlet spike position on engine stall limit. Free-stream Mach number, 2.0.

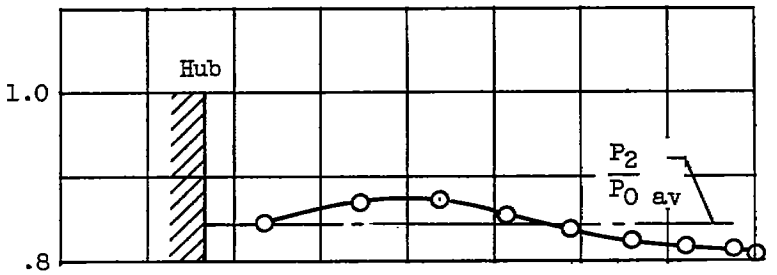

(a) Mach number at which conical shock intersects cowl lip, 1.8; compressor pressure ratio, 2.70; compressor-face total-pressure distortion, 0.08; no stall.

Compressor-face total-pressure ratio, P_2/P_0

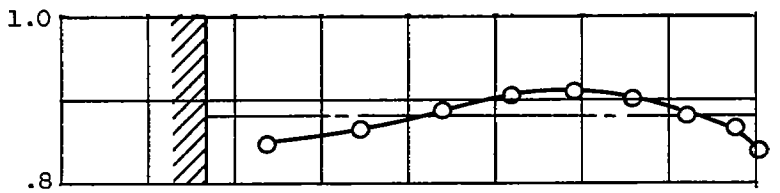

(b) Mach number at which conical shock intersects cowl lip, 1.9; compressor pressure ratio, 2.57; compressor-face total-pressure distortion, 0.09; stall.

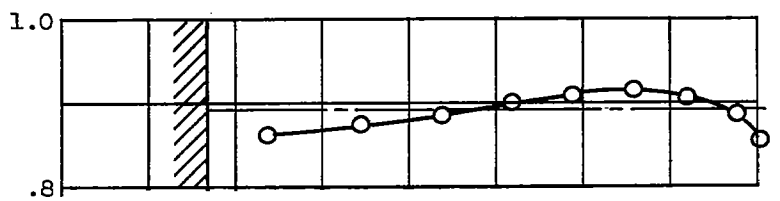

(c) Mach number at which conical shock intersects cowl lip, 2.0; compressor pressure ratio, 2.58; compressor-face total-pressure distortion, 0.08; stall.

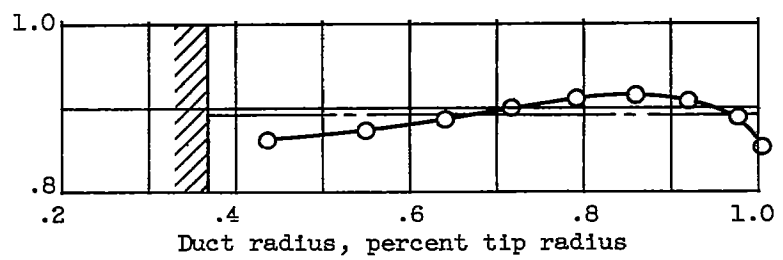

(d) Mach number at which conical shock intersects cowl lip, 2.1; compressor pressure ratio, 2.58; compressor-face total-pressure distortion, 0.08; stall.

Figure 13. - Effect of inlet spike position on compressor-face total-pressure profile. Free-stream Mach number, 2.0.

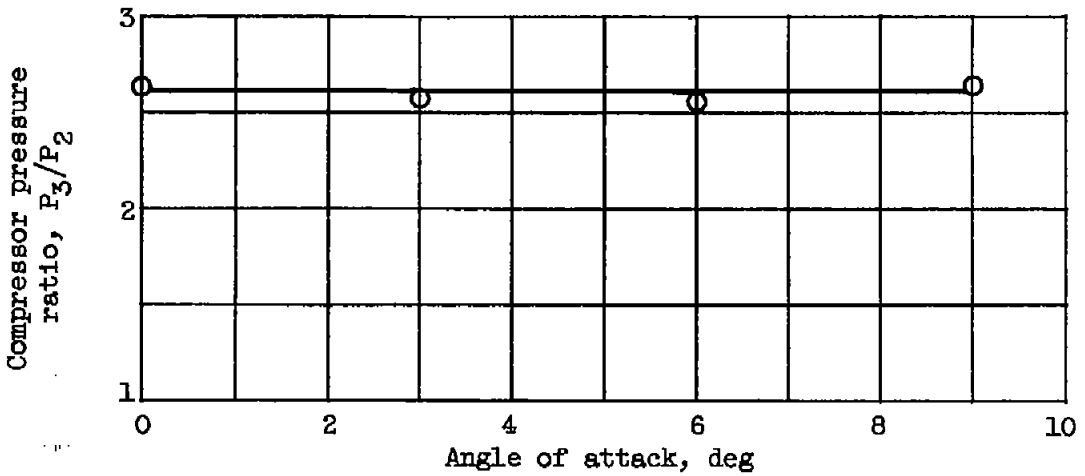

Figure 14. - Effect of angle of attack on compressor stall limit. Mach number at which conical shock intersects cowl lip, 2.4; free-stream Mach number, 2.0.

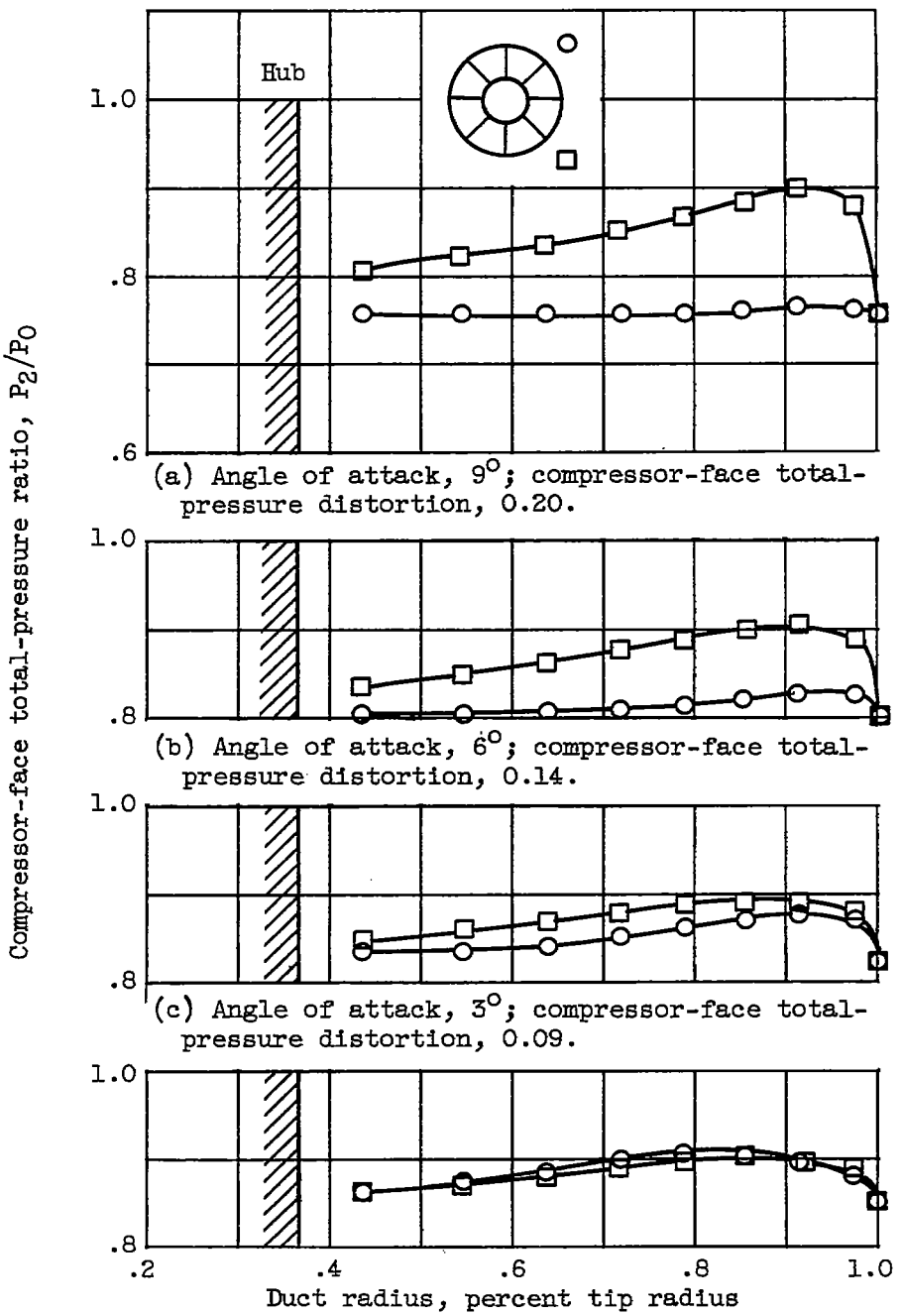

(a) Angle of attack, 9°; compressor-face total-pressure distortion, 0.20.

(b) Angle of attack, 6°; compressor-face total-pressure distortion, 0.14.

(c) Angle of attack, 3°; compressor-face total-pressure distortion, 0.09.

(d) Angle of attack, 0°; compressor-face total-pressure distortion, 0.07.

Figure 15. - Effect of angle of attack on compressor-face total-pressure profile. Mach number at which conical shock intersects cowl lip, 2.4; free-stream Mach number, 2.0.

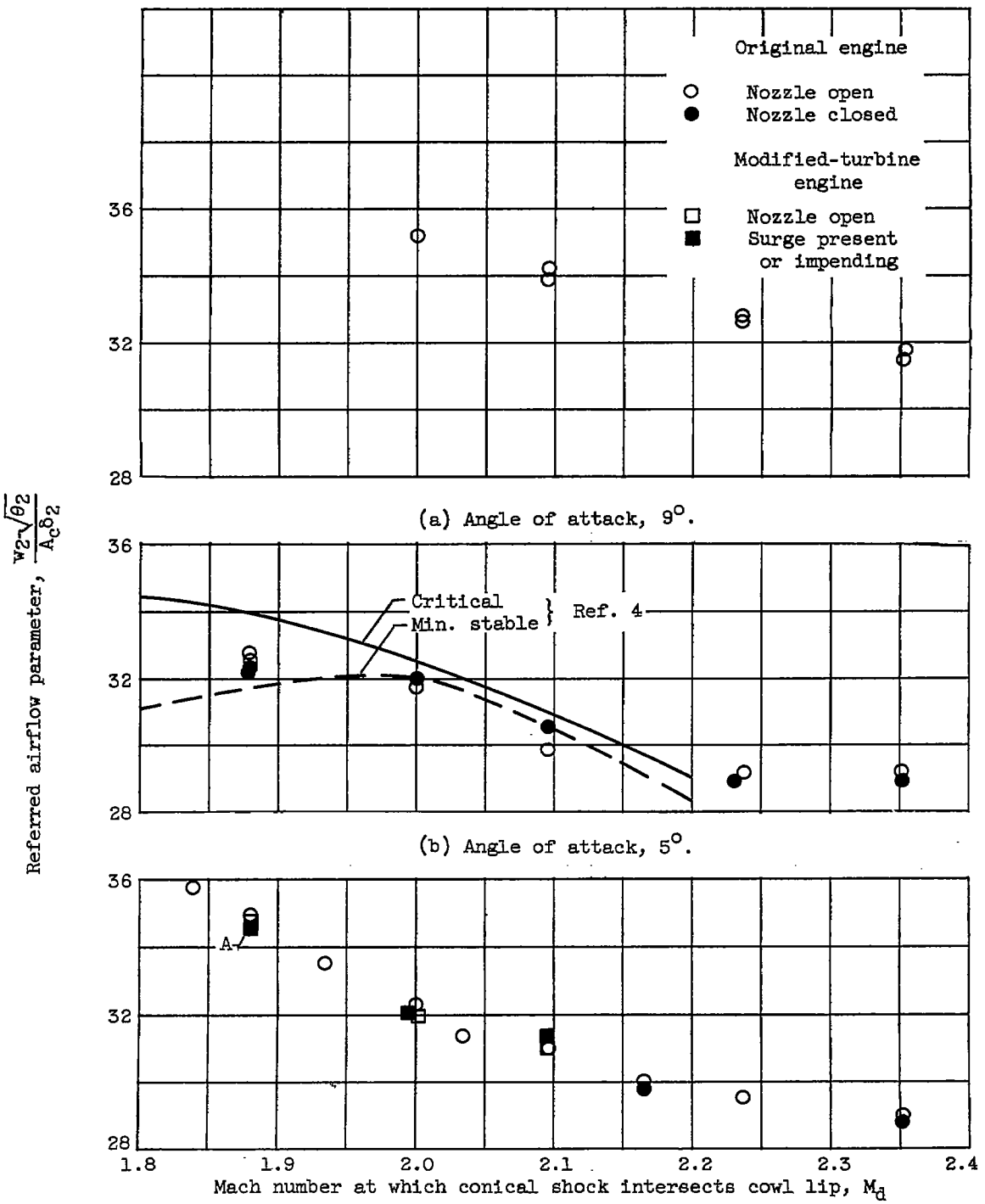

(a) Angle of attack, 9°.

(b) Angle of attack, 5°.

(c) Angle of attack, 0°.

Figure 16. - Effect of engine operation at or near stall on buzz limits of 25° cone inlet. Free-stream Mach number, 2.0.

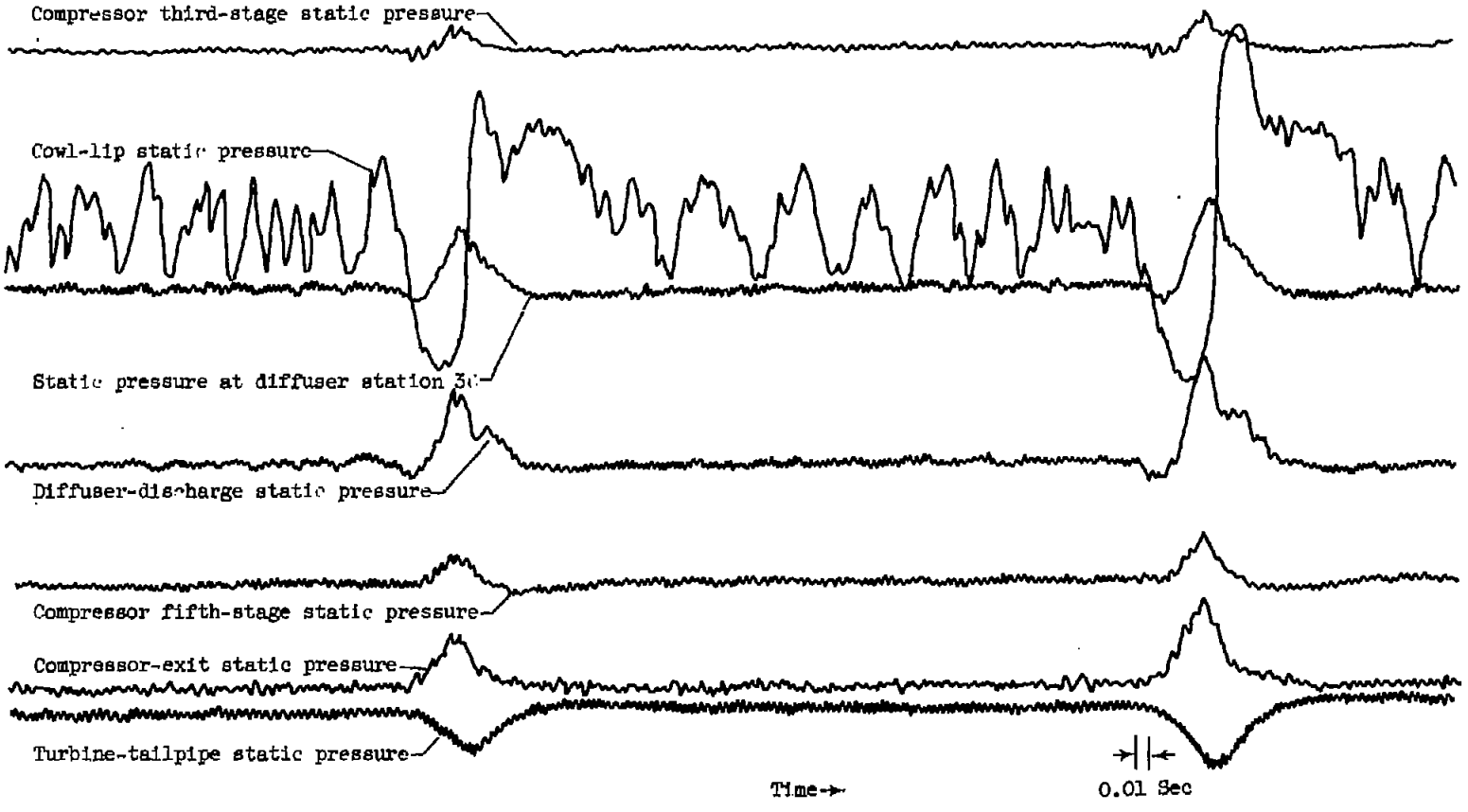

Figure 17. - Oscillogram of inlet-engine variables during compressor surge and light buzz. Mach number at which conical shock intersects cowl lip, 1.88; free-stream Mach number, 2.0; referred engine speed ratio, 0.808; compressor pressure ratio, 2.57.

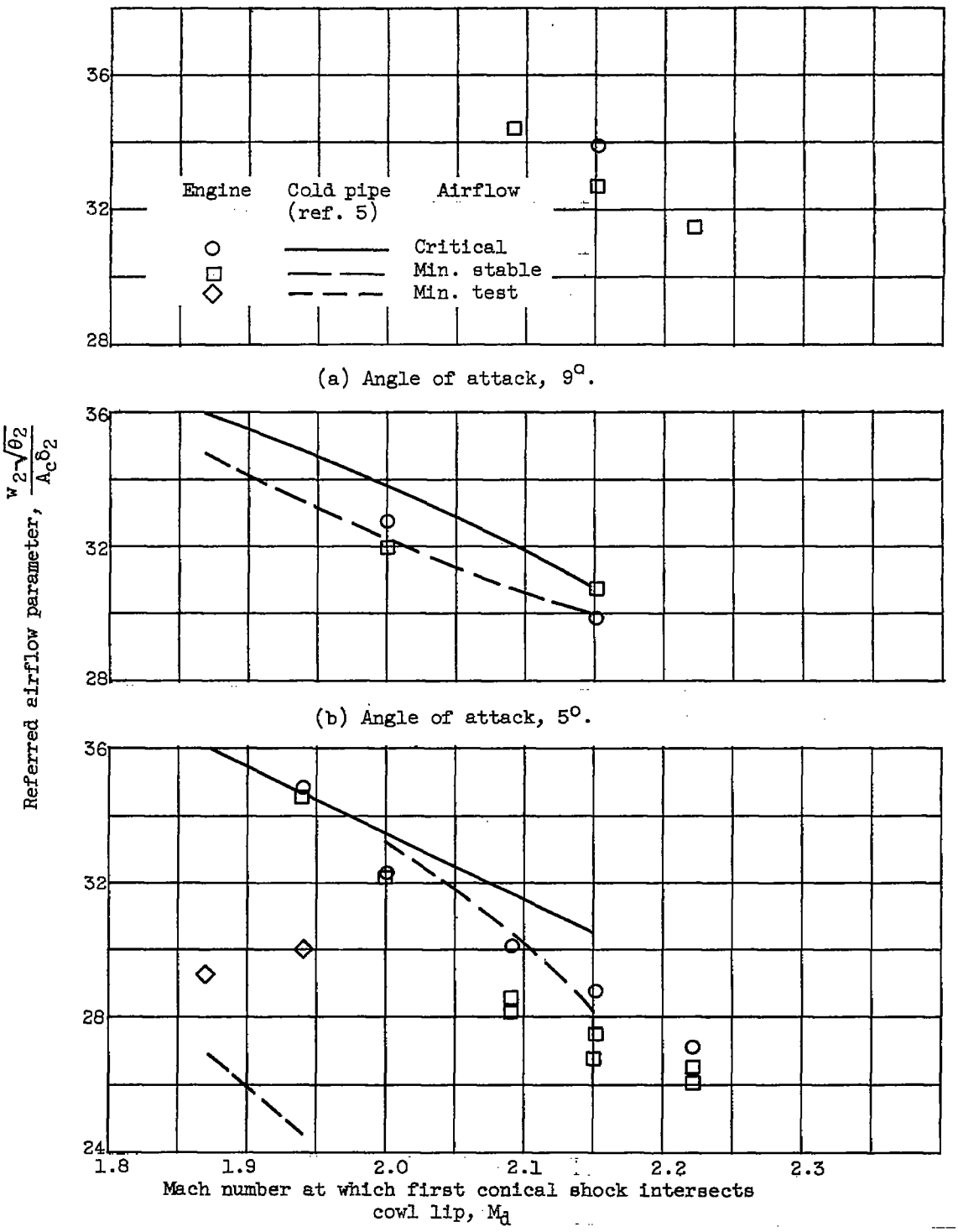

(a) Angle of attack, 9°.

(b) Angle of attack, 5°.

(c) Angle of attack, 0°.

Figure 18. - Effect of engine on buzz limits of 15° plus 10° double-cone inlet. Free-stream Mach number, 2.0.